Knockout of Syntaxin-4 in 3T3-L1 adipocytes reveals new insight into GLUT4 trafficking and adiponectin secretion

Hannah L. Black[1,*], Rachel Livingstone[2,*], Cynthia C. Mastick[2,3,*], Mohammed Al Tobi[2], Holly Taylor[4], Angéline Geiser[4], Laura Stirrat[4], Dimitrios Kioumourtzoglou[1], John R. Petrie[5], James G. Boyle[5,6], Nia J. Bryant[1,#] and Gwyn W. Gould[4,#]

[1]Department of Biology and York Biomedical Research Institute, University of York. Heslington, York, YO10 5DD UK.

[2]Henry Welcome Laboratory for Cell Biology, Institute for Molecular, Cellular and Systems Biology, College of Medical Veterinary and Life Sciences, University of Glasgow, Glasgow G12 8QQ. UK.

[3]Department of Biology, University of Nevada Reno, 1664 N. Virginia Street, Reno, NV 89557, USA.

[4]Strathclyde Institute for Pharmacy and Biomedical Sciences, 161 Cathedral Street, University of Strathclyde, Glasgow G4 0RE. UK.

[5]Institute of Cardiovascular and Medical Sciences, and [6]School of Medicine, Dentistry and Nursing, University of Glasgow. Glasgow G12 8QQ. UK.

*joint contribution.

[#]joint communicating authors: gwyn.gould@strath.ac.uk or nia.bryant@york.ac.uk

Abbreviations.

2DG: 2-deoxy-D-glucose; GLUT4: glucose transporter-4; GSC: GLUT4 storage compartment; IRAP: insulin-responsive aminopeptidase; IRV: insulin responsive GLUT4 containing vesicles; PM: plasma membrane; SNARE: Soluble N-ethylmaleimide-sensitive factor attachment protein receptors; t-SNARE: target-SNARE protein; v-SNARE: vesicle-SNARE protein; SM: Sec1/Munc18 protein; Sx: Syntaxin; *Syn4*: Sx4 gene;

Abstract

Adipocytes are key to metabolic regulation, exhibiting insulin-stimulated glucose transport which is underpinned by the insulin-stimulated delivery of glucose transporter-4 (GLUT4)-containing vesicles to the plasma membrane where they dock and fuse increasing cell surface GLUT4 levels. Adipocytokines such as adiponectin are secreted via a similar

mechanism. We used genome editing to knockout Syntaxin-4 a protein reported to mediate GLUT4-vesicle fusion with the plasma membrane in 3T3-L1 adipocytes. Syntaxin-4 knockout reduced insulin-stimulated glucose transport and adiponectin secretion by ~50% and reduced GLUT4 levels. Ectopic expression of HA-GLUT4-GFP showed that Syntaxin-4 knockout cells retain significant GLUT4 translocation capacity demonstrating that Syntaxin-4 is dispensable for insulin-stimulated GLUT4 translocation. Analysis of recycling kinetics revealed only a modest reduction in the exocytic rate of GLUT4 in knockout cells, and little effect on endocytosis. These analyses demonstrate that Syntaxin-4 is not always rate limiting for GLUT4 delivery to the cell surface. In sum, we show that Syntaxin-4 knockout results in reduced insulin-stimulated glucose transport, depletion of cellular GLUT4 levels and inhibition of adiponectin secretion but has only modest effects on the translocation capacity of the cells.

Introduction

Adipocytes exhibit a range of membrane trafficking events linked to the regulation of energy metabolism and glucose homeostasis. Best characterised amongst these is the insulin-stimulated delivery of glucose transporters (GLUT4) to the surface (Gould et al., 2020; Klip et al., 2019) and the constitutive secretion of a range of hormones, known collectively as adipocytokines (Fasshauer and Blüher, 2015; Lehr et al., 2012). As perturbation in either of these processes can lead to metabolic dysfunction (Carvalho et al., 2005; Graham and Kahn, 2007; Kahn, 2019; Kumar et al., 2010), identifying the mechanisms involved in the regulation of their exocytosis (or trafficking) is an important research goal.

Membrane trafficking between subcellular compartments, including the plasma membrane (PM) involves well-conserved molecular families that operate across species. One notable example is the SNARE (Soluble N-ethylmaleimide-sensitive factor attachment protein receptors) protein family (Wang et al., 2017). Members of this family localised on the target (tSNARE) and vesicle (vSNARE) membranes bind and assemble to form a complex that provides the energy to drive fusion (McNew et al., 2000; Weber et al., 2000). Cognate pairing of v- and tSNAREs can drive fusion providing an impetus to identify the SNAREs involved in GLUT4 delivery to the cell surface (Bryant and Gould, 2011; Olson et al., 1997).

A large body of experimental evidence has indicated a key role for Syntaxin-4 (Sx4) in GLUT4 trafficking. Introduction of anti-Sx4 into permeabilised adipocytes inhibited insulin-stimulated deoxyglucose (2DG) uptake by about 50% whereas a non-specific antibody was without effect (Volchuk et al., 1996); similarly GST-Sx4 was found to inhibit the appearance of GLUT4 in plasma membrane lawns in 3T3-L1 adipocytes (Cheatham et al., 1996), an effect not observed with GST-Sx3 (Olson 1997). A 50% inhibition of insulin-stimulated GLUT4 translocation was also observed using microinjection of peptides corresponding to regions 106-122 of Sx4 but not Sx1, suggesting that disruption of the interaction between Sx4 and other components of the cognate SNARE complex impairs GLUT4 translocation (Macaulay et al., 1997).

Homozygotic disruption of the *Syn4* gene in mice is embryonically lethal, but heterozygous *Syn4*$^{+/-}$ mice exhibit a roughly 50% diminution in whole body glucose uptake; an effect which parallels the ~50% reduction in skeletal muscle GLUT4 translocation (Yang et al., 2001). These data are strongly supportive of a role for Sx4 in GLUT4 translocation in skeletal muscle, but it is of interest that *Syn4*$^{+/-}$ mice exhibited normal insulin-stimulated glucose transport in adipocytes despite a 50% reduction in Sx4 protein (Yang et al., 2001). This is unlikely to be explained by an excess of Sx4, as studies in 3T3-L1 adipocytes and cardiomyocytes indicate that Sx4 is expressed at broadly the same levels as the other SNARE components identified as being involved in GLUT4 vesicle fusion with the cell surface (VAMP2 and SNAP23) (Bowman et al., 2019; Hickson et al., 2000). Further support for an important role for Sx4 is provided by studies of transgenic mice overexpressing Sx4 (Spurlin et al., 2004). These mice exhibit enhanced skeletal muscle glucose transport but did not display significantly increased glucose uptake in adipose tissue. Using siRNA knockdown of VAMP2, SNAP23 and Sx4 in 3T3-L1 adipocytes reduced insulin-stimulated glucose transport by around 50% in 3T3-L1 adipocytes (Kawaguchi et al., 2010). This study did suggest a requirement for Sx4 in tethering GLUT4-containing vesicles at the cell surface, but this was not assessed in living cells (Kawaguchi et al., 2010). A role for Sx4 is also supported by numerous studies which indicate that Sx4 and its cognate Sec1/Munc18 (SM) protein, Munc18c, play pivotal roles in the regulation of GLUT4 delivery to the cell surface (D'Andrea-Merrins et al., 2007; Kanda et al., 2005; Kioumourtzoglou et al., 2014; Oh et al., 2005; Tamori et al., 1998; Thurmond and Pessin, 2000; Thurmond et al., 1998, 2000). Collectively, these data support a role for Sx4 in GLUT4 translocation, particularly in skeletal muscle.

Many of the studies noted above exhibited only partial inhibition (Cheatham et al., 1996; Kawaguchi et al., 2010; Olson et al., 1997; Volchuk et al., 1996); this may be attributed to limitations in experimental systems and/or assay sensitivity, but the possibility that other mechanism(s) exist and act in parallel or in a compensatory fashion has not been addressed. The notable distinctions in the behaviour of adipose and muscle tissue in transgenic mice underscore the need to consider this possibility (Spurlin et al., 2004; Yang et al., 2001).

There is evidence that some SNARE-mediated trafficking events utilise functionally redundant SNAREs (Liu and Barlowe, 2002). Intriguingly, studies of the role of the vSNARE VAMP2 in insulin stimulated GLUT4 translocation revealed an unexpected plasticity (Zhao et al., 2009). Simultaneous disruption of VAMP2, 3 and 8 completely block insulin stimulated GLUT4 translocation in 3T3-L1 adipocytes; surprisingly this block could be overcome by re-expression of either VAMP2, 3 or 8 individually (Zhao et al., 2009). Such data prompted a re-evaluation of the role of Sx4 in GLUT4 translocation, particularly with the advent of genome editing and the ability to sensitively assay GLUT4 trafficking using epitope-tagged reporters. Because complete Sx4 knockout in mice is lethal (Yang et al., 2001), we undertook genome editing to knockout Sx4 in 3T3-L1 adipocytes in order to test the hypothesis that Sx4 is not be the only plasma membrane t-SNARE involved in GLUT4 translocation. We find that Sx4-knockout cells do not exhibit a change in insulin sensitivity but exhibit a reduced rate of insulin-stimulated 2DG transport which can be accounted for by reduced total cellular GLUT4 levels. A similar reduction in adiponectin secretion was also observed. Kinetic analysis of translocation of ectopically

expressed HA-GLUT4-GFP indicates that while loss of Sx4 decreases the maximal rate of GLUT4 trafficking, Sx4 depletion is not rate-limiting for GLUT4 delivery to the PM. We conclude that a further mechanism, in addition to Sx4, can mediate GLUT4-vesicle fusion with the plasma membrane of adipocytes, but that Sx4 plays a key role in the maintenance of cellular GLUT4 levels and in adiponectin secretion.

Results

Generation of Sx4 knockout cells. We used genome editing to knockout Sx4 in 3T3-L1 fibroblasts. Multiple lines of Sx4 knockouts were established and knockout of Sx4 confirmed by immunoblot analysis. DNA sequence analysis of two independent clones confirmed frameshift mutations, one after amino acid 23 the other at residue 24 of Sx4. In all that follows, at least three biological replicates of all experiments were performed on one clone, and the data confirmed using a second independent clone. We found that the Sx4 knockout cells differentiated into adipocytes as evidenced by the accumulation of visible lipid droplets, by expression of adipocyte-specific marker proteins including PPARγ (Figure 1A), and by Oil red-O staining (Figure 1B). Furthermore, we observe robust insulin-stimulated phosphorylation of Akt and ERK in Sx4 knockout cells at levels comparable to those observed in wildtype cells (Figure 1C). Analysis of plasma membrane associated SNARE proteins confirmed the absence of Sx4 in these cells, with no changes in the levels or distribution of either Sx2 or Sx3 among the different membrane fractions analysed (Figure 2).

Sx4-knockout cells exhibit reduced insulin-stimulated glucose transport and lower GLUT4 levels. We assayed insulin-stimulated glucose transport in control and Sx4 knockout cells (Figure 3A). As shown, Sx4 knockout cells exhibited a reduction in 2DG uptake. At 100nM insulin wild-type cells exhibited a 10.7 + 3.9-fold increase in 2DG uptake, but at the same insulin concentration, Sx4 knockout cells exhibited a 5.3 + 0.8-fold increase. Similar reductions were observed at lower insulin concentrations (see figure 3A), but the half maximal concentration was not significantly different between control and Sx4 wild-type cells, indicating that the effect was not a consequence of impaired insulin signalling. No difference in basal (unstimulated) rates of 2DG uptake were observed between wild-type and Sx4 knockout cells. The half-time of the rate of increase in insulin-stimulated 2DG uptake at 100nM insulin was unchanged upon Sx4 knockdown (not shown but see further examination of this point below). Sx4 knockdown was associated with a 54 + 3% reduction in total GLUT4 content (Figure 3B,C). This reduction was found mainly in the 16,000 xg supernatant, a fraction known to be enriched in the GLUT4 storage compartment (GSC) and insulin-responsive GLUT4-containing vesicles (IRV) which translocate to the cell surface in response to insulin; similar decreases in GLUT1 levels in this fraction were noted. By contrast, IRAP levels were unchanged. This suggests that the reduction insulin-stimulated 2DG can be explained by a reduction in GLUT4 levels. This was confirmed using the GLUT-specific inhibitor BAY-876. At low concentrations (~20nM), this compound is selective for GLUT1; at higher concentrations (2μM), both GLUT1 and GLUT4 are inhibited. Figure 3D confirms that in wild-type 3T3-L1 adipocytes, 43 + 24% of insulin-stimulated 2DG uptake is inhibited by 20nM BAY-876 suggesting that

60% of insulin-stimulated glucose transport in wild-type cells is GLUT4-dependent. In Sx4 knockout cells, essentially insulin-stimulated 2DG uptake is inhibited by 85 + 16% in the presence of 20nM BAY-876, a result consistent with the hypothesis that in Sx4 knockout cells, the majority of insulin-stimulated 2DG uptake is GLUT1-dependent.

Previous work from our group has shown that knockdown of Sx6 or Sx16 abrogates GLUT4 sorting into insulin responsive vesicles (IRV) and results in a decrease in total cell GLUT4 levels (Perera et al., 2003; Proctor et al., 2006). Similarly, an important role for Sortilin in GLUT4 trafficking has also been proposed (Huang et al., 2013; Pan et al., 2017, 2019). We therefore examined the levels of these proteins to test the hypothesis that knockout of Sx4 had in some way altered the machinery required for GLUT4 sequestration into the GSC/IRV. Figure 4 shows that neither the levels nor the distribution of Sx16 or Sortilin are altered in Sx4 knockout cells compared to wild-type cells. A small reduction in total Sx6 was observed in whole cell lysates, but analysis of the distribution of this SNARE among the subcellular fractions did not reveal any significant changes.

Adiponectin secretion is impaired in Sx4 knockout cells. 3T3-L1 adipocytes secrete a range of adipocytokines via the delivery of secretory cargo to the cell surface. We therefore tested whether Sx4 knockout affected adiponectin secretion. To quantify this, we used an adiponectin ELISA assay and in two separate platings of cells found that secretion of this protein was reduced by 50% upon Sx4 knockout (Figure 5A). This was accompanied by increased total cell adiponectin levels, as revealed by immunoblot analysis (Figure 5B,C). Thus, the reduction in adiponectin secretion arises from defective exocytosis of the protein rather than an effect on its expression or stability.

HA-GLUT4-GFP recycling reveals that the translocation machinery is largely intact. Our data indicate that Sx4 knockout cells exhibit reduced rates of insulin-stimulated glucose transport via a mechanism involving a reduction in total cell GLUT4 levels (discussed further below). We therefore decided to examine the effect of re-expression of GLUT4 in these cells, using the well-characterised HA-GLUT4-GFP (Muretta et al., 2007, 2008), and analysing kinetics of its trafficking using the model shown in Figure 6A (Habtemichael et al., 2011; Muretta and Mastick, 2009; Muretta et al., 2008). In the experiments that follow, levels of expression of HA-GLUT4-GFP were routinely too low to be easily quantified by immunoblotting; these conditions were chosen so as to minimise potential over-expression artefacts (Brewer et al., 2019; Habtemichael et al., 2011; Muretta et al., 2007, 2008). The data obtained are shown in Figure 6, where experiments in Sx4 knockout cells are compared to wild-type 3T3-L1 adipocytes expressing similar amounts of the HA-GLUT4-GFP, as judged by GFP intensity. Figure 6B shows that Sx4 knockout cells exhibit a 30% reduction in the maximal level of insulin-stimulated HA-GLUT4-GFP at the plasma membrane (PM in Figure 6A). In both cell types there was a robust translocation of GLUT4 in response to insulin (25-fold and 22-fold relative to basal levels in the two cell lines). This was not accompanied by an alteration in the EC_{50} of the insulin response (Figure 6C; 0.54 v 0.57nM, respectively), consistent with the transport data in Figure 3. Assay of the kinetics of GLUT4 recycling revealed that this is largely explained by a 50% reduction in the rate constant of exocytosis k_{ex} (Figure 6D). To test this, we assayed wortmannin-driven endocytosis of surface-labelled HA-GLUT4-GFP the rate of which was found to be identical between control and Sx4 knockout cells (Figure 6E).

These measured rate constants when fitted to the model shown in Figure 6A predict a 30% decrease in insulin-stimulated GLUT4 levels at the PM in Sx4 knockout cells relative to control cells, as observed (PM_{calc}; Figure 6F). Interestingly, examination of the time-course of the basal to insulin transition provides further insight (Figure 6F): the half-time of the increase in relative surface GLUT4 was not significantly changed in Sx4 knockout cells relative to wild-type cells (Figure 6F), consistent with the transition time course for insulin-stimulated glucose transport (data not shown). This finding is in marked contrast to that which would be predicted if Sx4 is rate limiting for the fusion of IRVs to the PM in response to insulin (shown by the dashed line in 6F) and suggests that the observed slow-down in GLUT4 exocytosis in Sx4 knockout cells is occurring at a different intracellular trafficking step. This is discussed further below.

Discussion.

Sx4 knockout perturbs GLUT4 levels and impairs secretion.

There is considerable experimental data supporting a role for Sx4 in the insulin-stimulated delivery of GLUT4 to the PM of muscle and adipocytes (Kawaguchi et al., 2010; Kioumourtzoglou et al., 2014; Olson et al., 1997; Tamori et al., 1998; Volchuk et al., 1996; Widberg et al., 2003; Yang et al., 2001). It is notable that many of these studies revealed a significant fraction of insulin-stimulated glucose transport and/or GLUT4 translocation remained after inhibition/knockdown of Sx4, hinting that other mechanisms may also be involved in this process. To address this, we generated Sx4 knockout 3T3-L1 cell lines and found that they exhibit a 50% reduction in insulin-stimulated glucose transport compared to wild-type cells but with an unchanged EC_{50} for insulin (Figure 3A). We found that this effect could largely be explained by a corresponding reduction in GLUT4 levels. It is perhaps worth noting here that a previous study of Sx4 knockdown in adipocytes did not examine this point (Kawaguchi et al., 2010). Using a simple fractionation procedure, we observed that this reduction was largely confined to a fraction known to be enriched in the GSC/IRV (Figure 3B,C). Using the GLUT-selective inhibitor BAY-876, we showed that in Sx4 knockout cells, the overwhelming majority of insulin-stimulated 2DG uptake is inhibited by 20nM BAY-876, compared to a 40% in wild-type cells (Figure 3D). At this concentration, BAY-876 is GLUT1-selective (Siebeneicher et al., 2016) hence this data argues that upon Sx4 knockout, GLUT1 is the major transporter active in these cells, consistent with the reduction in GLUT4 levels in the GSC/IRV-enriched fraction. Strikingly, the levels and distribution of IRAP and Sx16/Sx6 are unchanged upon Sx4 knockdown (Figure 4). These proteins play important roles in the trafficking of GLUT4 into the IRV (Gould et al., 2020; Perera et al., 2003; Proctor et al., 2006; Ross et al., 1998; Shewan et al., 2003; Watson et al., 2008; Yeh et al., 2007), suggesting that at least some components of the machinery for this remain largely intact. This will be returned to below.

Adipocytes secrete many small adipocytokines which act in an autocrine and paracrine fashion to regulate whole body energy metabolism (Kahn, 2019; Minokoshi et al., 2003). We observed a significant reduction in adiponectin secretion in Sx4 knockout cells, with an accompanying increase in total cell adiponectin levels (Figure 5). These observations are consistent with a reduction in exocytic events for secretory cargo in cells lacking Sx4. These data are, to our knowledge, the first to implicate Sx4 in adiponectin secretion; effects on other adipocytokines, such as leptin or adipsin, will be worthy of future experiments to ascertain whether this is a global (all adipocytokines) or protein-selective effect. It is again notable though that the reduction in secretion is only partial, suggesting that compensatory/alternative pathways for delivery of adiponectin-containing vesicles to the PM operate in these cells. Nevertheless, these data argue that Sx4 plays multiple roles in adipocyte biology.

Ectopic GLUT4 translocation in the absence of Sx4.

To dissect further the role of Sx4 in GLUT4 trafficking we used ectopic expression of HA-GLUT4-GFP; the presence of GLUT at the cell surface can be quantified by antibodies directed against the HA-epitope (present in the exofacial loop of GLUT4) and total GLUT4 levels assessed via the GFP tag (Blot and McGraw, 2006; Habtemichael et al., 2011; Karylowski et al., 2004; Martin et al., 2006; Muretta et al., 2007, 2008). Here we found that maximal insulin-stimulated GLUT4 translocation was only modestly impaired in Sx4 knockout cells (Figure 6B) and that the EC_{50} was unchanged (Figure 6C) compared to wild-type cells expressing comparable levels of HA-GLUT4-GFP. Thus, despite the complete absence of Sx4, a substantial translocation of GLUT4 was observed (typically >22-fold compared to 25-fold in control cells; Figure 6B), indicating that these cells have machinery capable of delivering GLUT4 to the PM in response to insulin. This conclusion is further supported by our observation that IRAP exhibits robust insulin-stimulated translocation in Sx4 knockout cells as assessed by subcellular fractionation (Supplemental figure 1). We used the HA-epitope to further examine the recycling properties of GLUT4 in these cells and interpret the results within the framework of an established recycling model shown in Figure 6A (Habtemichael et al., 2011; Muretta et al., 2007, 2008). These analyses revealed that Sx4 knockout is accompanied by a 50% reduction in the rate constant for exocytosis k_{ex} with no effect on the endocytic k_{en} (Figure 6D). Examination of the kinetics of the basal to insulin-stimulated transition (Figure 6F) revealed that although there is a significant inhibition of k_{ex}, the phenotype of these cells is not that predicted if Sx4 was rate-limiting for the final fusion step of GLUT4-containing IRVs to the PM ($k_{fuseIRV;}$ the dashed line in Figure 6F). Hence, our data reveal that GLUT4 is able to readily access the PM in response to insulin, albeit with a slower rate of exocytosis.

There are several potential explanations for this. First, many studies have indicated a degree of plasticity in SNARE protein function where loss of one SNARE can be compensated for by the system using a different SNARE, or where multiple SNAREs can perform similar functions. This has been described for the v-SNAREs in GLUT4 translocation (Sadler et al., 2015; Zhao et al., 2009) and in the exocytosis of chromaffin granules in neuroendocrine cells (Borisovska et al., 2005). In some cases, loss of one

SNARE is accompanied by a compensatory up-regulation of a related SNARE e.g. loss of Sec22p in yeast is compensated for by up-regulation of Ykt6p (Liu and Barlowe, 2002). This does not appear to be the case here as levels of Sx2, 3 and 16/6 are unchanged. However, whether the machinery which normally regulates Sx4 assembly into SNARE complexes can 'hijack' Sx2 or Sx3 remains to be explored. Recent work argues that the assembly of a functional SNARE complex by cognate SNARE interactions is a point of convergence for many regulatory mechanisms, including SM proteins, tethering complexes, Rab proteins etc (Baker and Hughson, 2016). Hence the absence of one component of this regulatory network may be maintained by other means. In this regard it is important to note that the SM protein involved in regulation of Sx4-containing SNARE complexes in response to insulin, Munc18c, can also bind to Sx2 and 3 and accelerate fusion catalysed by these Sx's *in vitro* (Yu et al., 2013). Hence, it is possible that insulin-stimulated translocation of ectopic HA-GLUT4-GFP is mediated by this kind of mechanism, but with reduced efficiency. This may explain the only partial effects observed in previous studies in which Sx4 function is inhibited. Similar arguments can be can also explain the observed reduced in adiponectin secretion.

However, a second, not mutually exclusive, model of Sx4 function should be considered. We speculate that our data may indicate that in the absence of Sx4, GLUT4 is unable to efficiently access the GSC/IRV and instead is localised to the recycling endosomes. Under these conditions we would predict that ubiquitination of GLUT4 would result in its degradation and cellular levels would decline – a phenotype reported for example upon Rab14 knockdown (Reed et al., 2013), Sx16/6 depletion (Perera et al., 2003; Proctor et al., 2006), depletion of Tankyrase (Sadler et al., 2019) and knockdown of SORT1 knockdown (Mastick, unpublished). The reduction in GLUT4 levels within the GSC/IRV observed in our study (Figure 2C,D) indicates that Sx4 somehow plays a role in the intracellular trafficking of GLUT4. Previous studies identified an intracellular pool of Sx4, which exhibited a small but reproducible insulin-stimulated translocation to the PM. Sx4 has also been observed within GLUT4-positive intracellular vesicles (Millar et al., 1999; Olson et al., 1997; Volchuk et al., 1996), but the functional consequences of this remain largely unexplored. One interpretation of our data is that as well as mediating effects at the PM, Sx4 may function to control aspects of intracellular GLUT4 trafficking hitherto unappreciated.

It is important to note that data obtained from knockout cells do not rule out an important role for Sx4 in insulin-stimulated GLUT4 translocation (Kioumourtzoglou et al., 2014). It is possible that adaptive responses to Sx4 knockout have arisen which although responsive to insulin are less sensitive. Further studies are clearly required to pinpoint the insulin-sensitive mechanism(s) that regulate Sx4 function and the data presented above represent in-road to this end. In particular, the data presented here reveal an important role for Sx4 in the maintenance of steady-state GLUT4 levels in 3T3-L1 adipocytes and begins to define the molecular machinery underpinning adipocytokine secretion.

Materials and Methods.

3T3-L1 cell culture and CRISPR genome editing. 3T3-L1 adipocytes, purchased from the American Tissue Culture Collection (#CL-173) were grown, maintained and differentiated exactly as outlined previously (Roccisana et al., 2013; Sadler et al., 2015) and confirmed to be free from mycoplasma by routine testing. Cells were used between 10 and 14 days after induction of differentiation and were serum-starved for 2h prior to all assays.

A CRISPR/Cas9 plasmid, targeting exon 2 of the Sx4 gene (Target ID: MM0000265990, targeting site 5'-GAGGTTCGAGTCGCGCTGGTGG-3') was purchased from Sigma Aldrich in the vector U6gRNA-Cas9-2A-RFP. The single vector expressed sgRNA, Cas9 nuclease and RFP. 3T3-L1 cells were transfected using GeneCellin as per manufacturer's instructions. 24 hours post transfection cells were trypsinised and pelleted at 800 rpm. Transfected cells were identified based on the presence of RFP fluorescence by sorting using a Beckman Coulter MoFlo Astrios flow cytometer and Summit 6.2 software. RFP positive cells were serially diluted, plated in 10 cm dishes and monitored for the growth of single colonies.

Once formed, single cell colonies were isolated by trypsinisation in colony rings. Colonies were expanded and Sx4 expression was screened using Immunoblotting and DNA sequencing. For sequencing, the genomic region surrounding the sgRNA targeting site was amplified using the following primers; Forward 5'- GCAACTGTCGCCAATGACTC-3', Reverse 5'- GAGGGGTTCCTCCTGAGACT-3'. Gel purified PCR products were sequenced using Eurofins Genomics' TubeSeq service, using the same primers. Sequences obtained from Sx4 knockout cells were compared to those from the equivalent DNA region amplified from 3T3-L1 WT cells.

Subcellular fractionation and immunoblotting. Adipocytes were homogenised and subjected to a subcellular fractionation protocol by successive centrifugation at 1000 x g to remove large debris and intact cells; some of the plasma membrane is also present within this fraction. This was followed by centrifugation at 16,000 x g. The Supernatant from this fraction has been shown to be enriched in GLUT4-containing vesicles (the GSC) (Sadler et al., 2016a, 2016b). The pellet contains dense membranes, including plasma membranes. Samples were resuspended in buffer for protein determination and analysed by SDS-PAGE and immunoblotting exactly as described (Sadler et al., 2015). Immunoblot signals were quantified exactly as outlined (Sadler et al., 2015). Data shown is from a minimum of three biological replicates for each antibody.

Antibodies used. Anti-Sx4 (#110042), Anti-Sx2 (#110022), Anti-Sx3 (#110032), Anti-Sx6 (#110062) and Anti-Sx16 (#110161) were from Synaptic Systems (Goettingen, Germany). Anti-GLUT1 (#652) and anti-GLUT4 (654) were from AbCam (Cambridge, United Kingdom) and anti-GAPDH (#4300) was from Ambion (Foster city, California, USA). Detection antibodies were from LI-COR Biosciences (Lincoln, Nebraska, USA). Anti-Sortilin (12369-1-AP), Anti-Tankyrase (18030-1-AP) and Anti-USP25 (12199-1-AP)

were from Proteintech. Anti-IRAP was from Paul Pilch (Boston College). Anti-ACRP30 was as described (Clarke et al., 2006).

Glucose transport. The accumulation of 2-deoxy-D-glucose (2DG) was assayed exactly as outlined (Roccisana et al., 2013). In these assays, the final concentration of 2DG was 50 μM, and an uptake time of 5 min was employed unless otherwise stated. Assays were performed in triplicate; nonspecific association of 2DG with the cells was determined using parallel assays containing 10μM cytochalasin B. Each experiment was replicated on at least three biological repeats of cells; in the case of the Sx4 knockout cells, the data was validated using two independent isolates of Sx4 knockout cells. For assays using the selective GLUT inhibitor BAY-876 (Sigma) (Siebeneicher et al., 2016), cells were incubated with this compound at the concentrations shown for 20 min prior to the addition of 2DG to initiate transport.

HA-GLUT4-GFP recycling and FACS analysis. Analysis of GLUT4 trafficking kinetics was as previously described (Brewer et al., 2016). Briefly, 3T3-L1 fibroblasts were infected with lentivirus encoding HA-GLUT4/GFP as described previously (Muretta et al., 2008). At the titres used, 70–80% of cells were infected and expressed the reporter protein; under these conditions, most of the infected cells will be infected with only one virion (Muretta et al., 2008). Cells were differentiated into adipocytes as described above in multi-well tissue culture plates. After labelling, the cells were placed on ice, removed from the plates by collagenase digestion, and single cell fluorescence analysed by flow cytometry. Insulin-sensitive, lipid droplet-filled adipocytes are identified based on light scatter (forward and side scatter) and cellular autofluorescence (488 excitation/>670 emission). Infected cells are distinguished from uninfected cells using GFP fluorescence; the uninfected cells in each sample were used as internal controls to measure background fluorescence from nonspecific antibody labelling and autofluorescence. Similar levels of GFP fluorescence were measured in wild-type and Sx4 knockout cells, indicating similar levels of HA-GLUT4-GFP expression was achieved in both cell types.

For all experiments, cells were serum-starved for 2 h at 37 °C in low serum media (LSM; 0.5% FBS in DMEM). Insulin was added to the LSM for the final 45 min of starvation in samples, or for increasing times as indicated on the figure legends. To label surface GLUT4, cells were placed on ice and incubated with 25μg/ml HA.11 monoclonal antibody (α-HA; Covance) that had been labelled with Alexa-Fluor 647 (AF647-α-HA) for 1 h (Brewer et al., 2016; Muretta et al., 2008). To measure GLUT4 uptake/recycling kinetics, cells were serum-starved in LSM ± insulin and then incubated at 37 °C in the continuous presence of AF647-α-HA in LSM ± insulin for increasing amounts of time. To estimate the rate constant of endocytosis, cells were pre-treated with insulin for 45 min as described above, then with wortmannin for increasing times. The GLUT4 remaining on the cell surface was then measured.

Adiponectin assays. For analysis of secreted proteins, adipocytes were washed gently four times with serum-free Dulbecco's modified Eagles Medium then incubated in serum-free media for 24h. The next day, the medium was carefully harvested, centrifuged at 50,000 xg for 30 minutes and the supernatant used in ACRP30 quantikine ELISA assay (#MRP300; from R&D Systems Inc.).

Statistical Analysis. Statistical testing was performed with GraphPad Prism 7. Where appropriate, the relevant statistical test that was implemented is reported in the figure legends. The level of significance was set at P=0.05.

Acknowledgments. This work was supported by grants from Diabetes UK (15/0005246, 17/0005605, 17/0005724,18/0005847, 18/0005905 and 19/0005978 to GWG and/or NJB), the Novo Nordisk Research Foundation (to GWG, JRP and JGB). AG thanks the Lister Institute for a summer research stipend and the EPSRC for a PhD studentship (AG). Mal-T thanks the Government of Oman for a studentship. CCM thanks the University of Nevada, Reno for sabbatical support. We thank Dr Peter Bowman for helpful discussions.

Bibliography

Baker, R.W., and Hughson, F.M. (2016). Chaperoning SNARE assembly and disassembly. Nat. Rev. Mol. Cell Biol. *17*, 465–479.

Blot, N., and McGraw, T.E. (2006). GLUT4 is internalised by a cholesterol-dependent nystatin-sensitive mechanism inhibited by insulin. EMBO J. *25*, 5648–5658.

Borisovska, M., Zhao, Y., Tsytsyura, Y., Glyvuk, N., Takamori, S., Matti, U., Rettig, J., Südhof, T., and Bruns, D. (2005). v-SNAREs control exocytosis of vesicles from priming to fusion. EMBO J. *24*, 2114–2126.

Bowman, P.R.T., Smith, G.L., and Gould, G.W. (2019). GLUT4 expression and glucose transport in human induced pluripotent stem cell-derived cardiomyocytes. PLoS One *14*, e0217885.

Brewer, P.D., Habtemichael, E.N., Romenskaia, I., Coster, A.C.F., and Mastick, C.C. (2016). Rab14 limits the sorting of Glut4 from endosomes into insulin-sensitive regulated secretory compartments in adipocytes. Biochem. J. *473*, 1315–1327.

Brewer, P.D., Romenskaia, I., and Mastick, C.C. (2019). A high-throughput chemical-genetics screen in murine adipocytes identifies insulin-regulatory pathways. J. Biol. Chem. *294*, 4103–4118.

Bryant, N.J., and Gould, G.W. (2011). SNARE proteins underpin insulin-regulated GLUT4 traffic. Traffic *12*, 657–664.

Carvalho, E., Kotani, K., Peroni, O.D., and Kahn, B.B. (2005). Adipose-specific overexpression of GLUT4 reverses insulin resistance and diabetes in mice lacking GLUT4 selectively in muscle. Am. J. Physiol. Endocrinol. Metab. *289*, E551-61.

Cheatham, B., Volchuk, A., Kahn, C.R., Wang, L., Rhodes, C.J., and Klip, A. (1996). Insulin-stimulated translocation of GLUT4 glucose transporters requires SNARE-complex proteins. Proc. Natl. Acad. Sci. USA *93*, 15169–15173.

Clarke, M., Ewart, M.-A., Santy, L.C., Prekeris, R., and Gould, G.W. (2006). ACRP30 is secreted from 3T3-L1 adipocytes via a Rab11-dependent pathway. Biochem. Biophys. Res. Commun. *342*, 1361–1367.

D'Andrea-Merrins, M., Chang, L., Lam, A.D., Ernst, S.A., and Stuenkel, E.L. (2007). Munc18c interaction with syntaxin 4 monomers and SNARE complex intermediates in GLUT4 vesicle trafficking. J. Biol. Chem. *282*, 16553–16566.

Fasshauer, M., and Blüher, M. (2015). Adipokines in health and disease. Trends Pharmacol. Sci. *36*, 461–470.

Gould, G.W., Brodsky, F.M., and Bryant, N.J. (2020). Building GLUT4 vesicles: CHC22 clathrin's human touch. Trends Cell Biol.

Graham, T.E., and Kahn, B.B. (2007). Tissue-specific alterations of glucose transport and molecular mechanisms of intertissue communication in obesity and type 2 diabetes. Horm Metab Res *39*, 717–721.

Habtemichael, E.N., Brewer, P.D., Romenskaia, I., and Mastick, C.C. (2011). Kinetic evidence that Glut4 follows different endocytic pathways than the receptors for transferrin and alpha2-macroglobulin. J. Biol. Chem. *286*, 10115–10125.

Hickson, G.R., Chamberlain, L.H., Maier, V.H., and Gould, G.W. (2000). Quantification of SNARE protein levels in 3T3-L1 adipocytes: implications for insulin-stimulated glucose transport. Biochem. Biophys. Res. Commun. *270*, 841–845.

Huang, G., Buckler-Pena, D., Nauta, T., Singh, M., Asmar, A., Shi, J., Kim, J.Y., and Kandror, K.V. (2013). Insulin responsiveness of glucose transporter 4 in 3T3-L1 cells depends on the presence of sortilin. Mol. Biol. Cell *24*, 3115–3122.

Kahn, B.B. (2019). Adipose Tissue, Inter-Organ Communication, and the Path to Type 2 Diabetes: The 2016 Banting Medal for Scientific Achievement Lecture. Diabetes *68*, 3–14.

Kanda, H., Tamori, Y., Shinoda, H., Yoshikawa, M., Sakaue, M., Udagawa, J., Otani, H., Tashiro, F., Miyazaki, J., and Kasuga, M. (2005). Adipocytes from Munc18c-null mice show increased sensitivity to insulin-stimulated GLUT4 externalization. J. Clin. Invest. *115*, 291–301.

Karylowski, O., Zeigerer, A., Cohen, A., and McGraw, T.E. (2004). GLUT4 is retained by an intracellular cycle of vesicle formation and fusion with endosomes. Mol. Biol. Cell *15*, 870–882.

Kawaguchi, T., Tamori, Y., Kanda, H., Yoshikawa, M., Tateya, S., Nishino, N., and Kasuga, M. (2010). The t-SNAREs syntaxin4 and SNAP23 but not v-SNARE VAMP2 are indispensable to tether GLUT4 vesicles at the plasma membrane in adipocyte. Biochem. Biophys. Res. Commun. *391*, 1336–1341.

Kioumourtzoglou, D., Gould, G.W., and Bryant, N.J. (2014). Insulin stimulates syntaxin4 SNARE complex assembly via a novel regulatory mechanism. Mol. Cell. Biol. *34*, 1271–1279.

Klip, A., McGraw, T.E., and James, D.E. (2019). Thirty sweet years of GLUT4. J. Biol. Chem. *294*, 11369–11381.

Kumar, A., Lawrence, J.C., Jung, D.Y., Ko, H.J., Keller, S.R., Kim, J.K., Magnuson, M.A., and Harris, T.E. (2010). Fat cell-specific ablation of rictor in mice impairs insulin-regulated fat cell and whole-body glucose and lipid metabolism. Diabetes *59*, 1397–1406.

Lehr, S., Hartwig, S., and Sell, H. (2012). Adipokines: a treasure trove for the discovery of biomarkers for metabolic disorders. Proteomics Clin Appl *6*, 91–101.

Liu, Y., and Barlowe, C. (2002). Analysis of Sec22p in endoplasmic reticulum/Golgi transport reveals cellular redundancy in SNARE protein function. Mol. Biol. Cell *13*, 3314–3324.

Macaulay, S.L., Hewish, D.R., Gough, K.H., Stoichevska, V., MacPherson, S.F., Jagadish, M., and Ward, C.W. (1997). Functional studies in 3T3L1 cells support a role for SNARE proteins in insulin stimulation of GLUT4 translocation. Biochem. J. *324 (Pt 1)*, 217–224.

Martin, O.J., Lee, A., and McGraw, T.E. (2006). GLUT4 distribution between the plasma membrane and the intracellular compartments is maintained by an insulin-modulated bipartite dynamic mechanism. J. Biol. Chem. *281*, 484–490.

McNew, J.A., Weber, T., Parlati, F., Johnston, R.J., Melia, T.J., Söllner, T.H., and Rothman, J.E. (2000). Close is not enough: SNARE-dependent membrane fusion requires an active mechanism that transduces force to membrane anchors. J. Cell Biol. *150*, 105–117.

Millar, C.A., Shewan, A., Hickson, G.R., James, D.E., and Gould, G.W. (1999). Differential regulation of secretory compartments containing the insulin-responsive glucose transporter 4 in 3T3-L1 adipocytes. Mol. Biol. Cell *10*, 3675–3688.

Minokoshi, Y., Kahn, C.R., and Kahn, B.B. (2003). Tissue-specific ablation of the GLUT4 glucose transporter or the insulin receptor challenges assumptions about insulin action and glucose homeostasis. J. Biol. Chem. *278*, 33609–33612.

Muretta, J.M., and Mastick, C.C. (2009). How insulin regulates glucose transport in adipocytes. Vitam Horm *80*, 245–286.

Muretta, J.M., Romenskaia, I., Cassiday, P.A., and Mastick, C.C. (2007). Expression of a synapsin IIb site 1 phosphorylation mutant in 3T3-L1 adipocytes inhibits basal intracellular retention of Glut4. J. Cell Sci. *120*, 1168–1177.

Muretta, J.M., Romenskaia, I., and Mastick, C.C. (2008). Insulin releases Glut4 from static storage compartments into cycling endosomes and increases the rate constant for Glut4 exocytosis. J. Biol. Chem. *283*, 311–323.

Oh, E., Spurlin, B.A., Pessin, J.E., and Thurmond, D.C. (2005). Munc18c heterozygous knockout mice display increased susceptibility for severe glucose intolerance. Diabetes *54*, 638–647.

Olson, A.L., Knight, J.B., and Pessin, J.E. (1997). Syntaxin 4, VAMP2, and/or VAMP3/cellubrevin are functional target membrane and vesicle SNAP receptors for insulin-stimulated GLUT4 translocation in adipocytes. Mol. Cell. Biol. *17*, 2425–2435.

Pan, X., Zaarur, N., Singh, M., Morin, P., and Kandror, K.V. (2017). Sortilin and retromer mediate retrograde transport of Glut4 in 3T3-L1 adipocytes. Mol. Biol. Cell *28*, 1667–1675.

Pan, X., Meriin, A., Huang, G., and Kandror, K.V. (2019). Insulin-responsive amino peptidase follows the Glut4 pathway but is dispensable for the formation and translocation of insulin-responsive vesicles. Mol. Biol. Cell *30*, 1536–1543.

Perera, H.K., Clarke, M., Morris, N.J., Hong, W., Chamberlain, L.H., and Gould, G.W. (2003). Syntaxin 6 regulates Glut4 trafficking in 3T3-L1 adipocytes. Mol. Biol. Cell *14*, 2946–2958.

Proctor, K.M., Miller, S.C.M., Bryant, N.J., and Gould, G.W. (2006). Syntaxin 16 controls the intracellular sequestration of GLUT4 in 3T3-L1 adipocytes. Biochem. Biophys. Res. Commun. *347*, 433–438.

Reed, S.E., Hodgson, L.R., Song, S., May, M.T., Kelly, E.E., McCaffrey, M.W., Mastick, C.C., Verkade, P., and Tavaré, J.M. (2013). A role for Rab14 in the endocytic trafficking of GLUT4 in 3T3-L1 adipocytes. J. Cell Sci. *126*, 1931–1941.

Roccisana, J., Sadler, J.B.A., Bryant, N.J., and Gould, G.W. (2013). Sorting of GLUT4 into its insulin-sensitive store requires the Sec1/Munc18 protein mVps45. Mol. Biol. Cell *24*, 2389–2397.

Ross, S.A., Keller, S.R., and Lienhard, G.E. (1998). Increased intracellular sequestration of the insulin-regulated aminopeptidase upon differentiation of 3T3-L1 cells. Biochem. J. *330 (Pt 2)*, 1003–1008.

Sadler, J.B.A., Bryant, N.J., and Gould, G.W. (2015). Characterization of VAMP isoforms in 3T3-L1 adipocytes: implications for GLUT4 trafficking. Mol. Biol. Cell *26*, 530–536.

Sadler, J.B.A., Lamb, C.A., Gould, G.W., and Bryant, N.J. (2016a). 16K Fractionation of 3T3-L1 Adipocytes to Produce a Crude GLUT4-Containing Vesicle Fraction. Cold Spring Harb. Protoc. *2016*, pdb.prot083683.

Sadler, J.B.A., Lamb, C.A., Gould, G.W., and Bryant, N.J. (2016b). Complete Membrane Fractionation of 3T3-L1 Adipocytes. Cold Spring Harb. Protoc. *2016*, pdb.prot083691.

Sadler, J.B.A., Lamb, C.A., Welburn, C.R., Adamson, I.S., Kioumourtzoglou, D., Chi, N.-W., Gould, G.W., and Bryant, N.J. (2019). The deubiquitinating enzyme USP25 binds tankyrase and regulates trafficking of the facilitative glucose transporter GLUT4 in adipocytes. Sci. Rep. *9*, 4710.

Shewan, A.M., van Dam, E.M., Martin, S., Luen, T.B., Hong, W., Bryant, N.J., and James, D.E. (2003). GLUT4 recycles via a trans-Golgi network (TGN) subdomain enriched in Syntaxins 6 and 16 but not TGN38: involvement of an acidic targeting motif. Mol. Biol. Cell *14*, 973–986.

Siebeneicher, H., Cleve, A., Rehwinkel, H., Neuhaus, R., Heisler, I., Müller, T., Bauser, M., and Buchmann, B. (2016). Identification and Optimization of the First Highly Selective GLUT1 Inhibitor BAY-876. ChemMedChem *11*, 2261–2271.

Spurlin, B.A., Park, S.-Y., Nevins, A.K., Kim, J.K., and Thurmond, D.C. (2004). Syntaxin 4 transgenic mice exhibit enhanced insulin-mediated glucose uptake in skeletal muscle. Diabetes *53*, 2223–2231.

Tamori, Y., Kawanishi, M., Niki, T., Shinoda, H., Araki, S., Okazawa, H., and Kasuga, M. (1998). Inhibition of insulin-induced GLUT4 translocation by Munc18c through interaction with syntaxin4 in 3T3-L1 adipocytes. J. Biol. Chem. *273*, 19740–19746.

Thurmond, D.C., and Pessin, J.E. (2000). Discrimination of GLUT4 vesicle trafficking from fusion using a temperature-sensitive Munc18c mutant. EMBO J. *19*, 3565–3575.

Thurmond, D.C., Ceresa, B.P., Okada, S., Elmendorf, J.S., Coker, K., and Pessin, J.E. (1998). Regulation of insulin-stimulated GLUT4 translocation by Munc18c in 3T3L1 adipocytes. J. Biol. Chem. *273*, 33876–33883.

Thurmond, D.C., Kankai, M., Khan, A.H., and Pessin, J.E. (2000). Munc18c function is required for insulin-stimulated plasma membrane fusion of Glut4 and insulin-responsive aminopeptidase storage vesicles. Mol. Cell. Biol. *20*, 379–388.

Volchuk, A., Wang, Q., Ewart, H.S., Liu, Z., He, L., Bennett, M.K., and Klip, A. (1996). Syntaxin 4 in 3T3-L1 adipocytes: Regulation by insulin and participation in insulin-dependent glucose transport. Mol. Biol. Cell. *7*, 1075–1082.

Wang, T., Li, L., and Hong, W. (2017). SNARE proteins in membrane trafficking. Traffic *18*, 767–775.

Watson, R.T., Hou, J.C., and Pessin, J.E. (2008). Recycling of IRAP from the plasma membrane back to the insulin-responsive compartment requires the Q-SNARE syntaxin 6 but not the GGA clathrin adaptors. J. Cell Sci. *121*, 1243–1251.

Weber, T., Parlati, F., McNew, J.A., Johnston, R.J., Westermann, B., Sollner, T.H., and Rothman, J.E. (2000). SNAREpins are functionally resistant to disruption by NSF and. J. Cell Biol. *149*, 1063–1072.

Widberg, C.H., Bryant, N.J., Girotti, M., Rea, S., and James, D.E. (2003). Tomosyn interacts with the t-SNAREs syntaxin4 and SNAP23 and plays a role in insulin-stimulated GLUT4 translocation. J. Biol. Chem. *278*, 35093–35101.

Yang, C., Coker, K.J., Kim, J.K., Mora, S., Thurmond, D.C., Davis, A.C., Yang, B., Williamson, R.A., Shulman, G.I., and Pessin, J.E. (2001). Syntaxin 4 heterozygous knockout mice develop muscle insulin resistance. J. Clin. Invest. *107*, 1311–1318.

Yeh, T.-Y.J., Sbodio, J.I., Tsun, Z.-Y., Luo, B., and Chi, N.-W. (2007). Insulin-stimulated exocytosis of GLUT4 is enhanced by IRAP and its partner tankyrase. Biochem. J. *402*, 279–290.

Yu, H., Rathore, S.S., Lopez, J.A., Davis, E.M., James, D.E., Martin, J.L., and Shen, J. (2013). Comparative studies of Munc18c and Munc18-1 reveal conserved and divergent mechanisms of Sec1/Munc18 proteins. Proc. Natl. Acad. Sci. USA *110*, E3271-80.

Zhao, P., Yang, L., Lopez, J.A., Fan, J., Burchfield, J.G., Bai, L., Hong, W., Xu, T., and James, D.E. (2009). Variations in the requirement for v-SNAREs in GLUT4 trafficking in adipocytes. J. Cell Sci. *122*, 3472–3480.

Figures

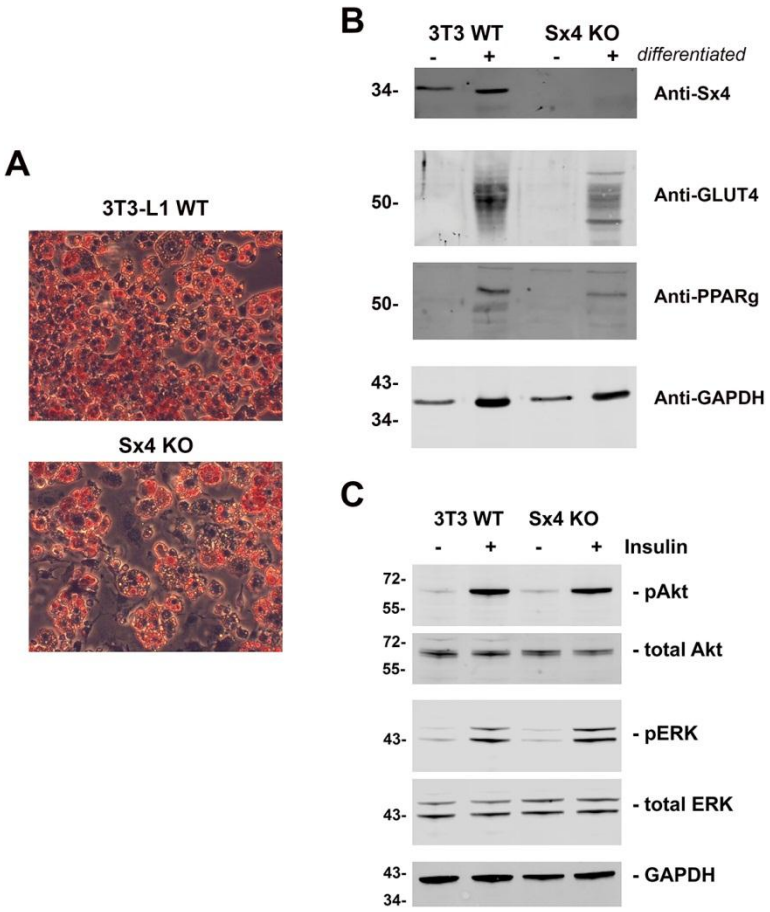

Figure 1. Characteristics of Sx4 knockout 3T3-L1 cells.

WT and Sx4 knockout (KO)3T3-L1 fibroblasts were treated with adipocyte differentiation media for 12 days. Panel ***A*** shows Oil-Red O staining of cells 12 days after differentiation. Panel ***B*** shows representative immunoblots of expression of the adipogenesis markers peroxisome proliferating factor (PPARγ) and GLUT4 which were increased following differentiation in both parental (3T3 WT) and Sx4 knockout (KO) lines. GAPDH is shown as a control, and Sx4 confirms the validity of the knockout lines. 15 μg of protein was loaded on each lane. Panel ***C*** compares basal and insulin-stimulated signalling proteins in parental (3T3 WT) and Sx4 knockout (KO) adipocytes at day 10. Cells were incubated in serum-free media for 2h prior to incubation with 100 nM insulin for 15 minutes. Lysates were immunoblotted for the proteins indicated. Data from a typical experiment is shown, repeated three times with qualitatively similar results; each lane contains 15 μg of protein.

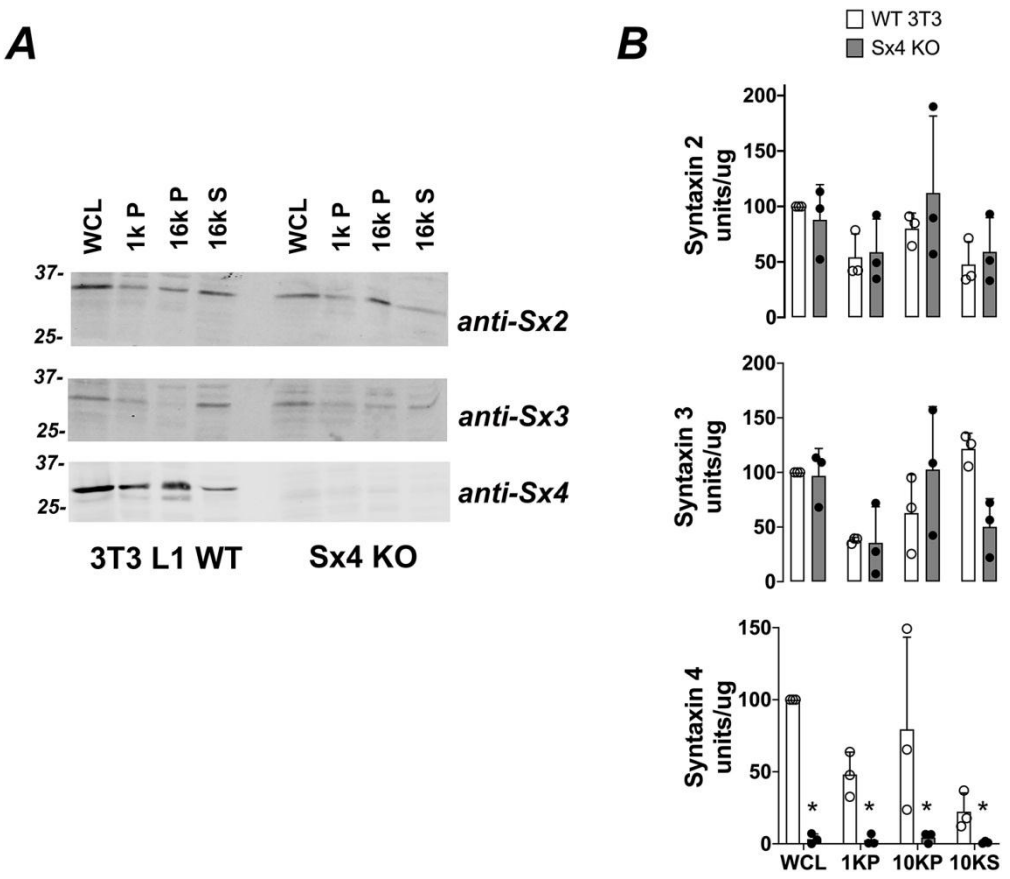

Figure 2 t-SNARE expression in Sx4 knockout adipocytes.

Panel ***A*** shows representative immunoblots of subcellular fractions from either wild-type or Sx4 knockout (KO) 3T3-L1 adipocytes probed for the indicated plasma membrane Syntaxin. WCL = whole cell lysate, 1kP is the pellet obtained after centrifugation at 1,000 x*g* which is enriched for large debris and contains some of the plasma membrane; the pellet obtained after centrifugation at 16,000 x*g*, designated 16kP, contains heavy microsomes and plasma membrane and the corresponding supernatant 16kS which contains light microsomes and is enriched for the GSC. Equal protein loads of each fraction were loaded on each lane. Panel ***B*** shows quantification of separate immunoblots of this type from three biological replicates comparing wild-type 3T3 L1 cells and Sx4 knockout. No differences in levels of Sx2 or Sx3 in any fraction were observed. Sx4 levels were significantly reduced in all fractions, *$p<0.02$ for all fractions.

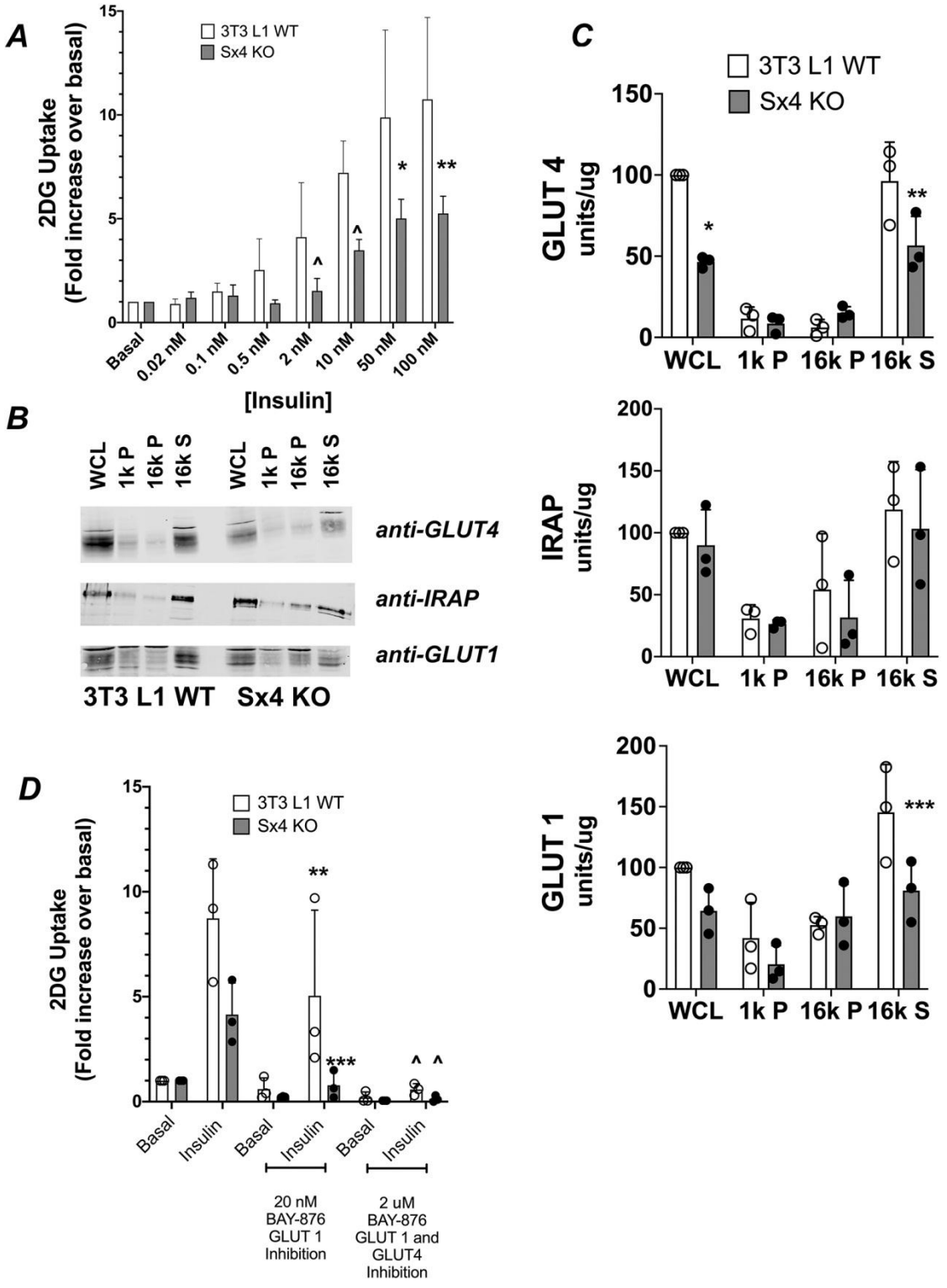

Figure 3 Insulin-stimulated glucose transport in Sx4 knockout cells.

Panel ***A***: Triplicate wells of cells treated with or without the indicated concentration of insulin for twenty minutes were used to assay 2-deoxy-D-glucose (2DG) uptake as described. Data was corrected for non-specific uptake of isotope with the cells by performing parallel assays in the presence of 10 μM cytochalasin B, and the data normalised to the rate assayed in the absence of insulin (basal) for each data set. Shown are the fold increases in 2DG uptake at the indicated concentrations expressed as a

mean and s.d. of at least three biological replicates. A significant difference between wild-type and Sx4 knockout cells was observed *p=0.01 at 50nM and **p=0.004 at 100nM, and a trend towards significance seen at 2 nm and 10nM (^p~0.09). Basal rates of 2DG uptake were not different between wild-type and Sx4 knockout cells. Panel ***B*** shows representative immunoblots of subcellular fractions (as described in the legend to figure 1) probed for GLUT4, GLUT1 and IRAP; equal amounts of each fraction were loaded per lane. Panel ***C*** shows quantification of at least three independent subcellular fractionation experiments quantified as described. Results were analysed by 2-way ANOVA. *p=0.001. **p=0.02, ***p=0.02. The different in GLUT1 levels in WCL did not reach statistical significance (p=0.16). Panel ***D*** shows the effect of the GLUT-specific inhibitor BAY-876 on 2DG uptake in basal and 100nM insulin-stimulated cells. Insulin-stimulated 2DG uptake was significantly lower in Sx4 knockout cells compared to wild-type cells (*p=0.006). In the presence of 20 nM BAY876, insulin-stimulated 2DG uptake in wild-type cells was inhibited by 42% (**p=0.05). However, 20nM BAY-876 completely abolished insulin-stimulated 2DG uptake in Sx4 knockout cells (***p=0.013 compared to insulin-stimulated 2DG uptake in Sx4 knockout cells in the absence of BAY876; this value was not significantly different to basal transport rate in this cell type). At 2μM BAY876, 2DG uptake was essentially completely abolished in both cell lines (^p~0.03, compared to corresponding values in the absence of BAY-876). Statistical analysis was performed using ANOVA in Prism; data from three independent experiments was analysed using each cell line.

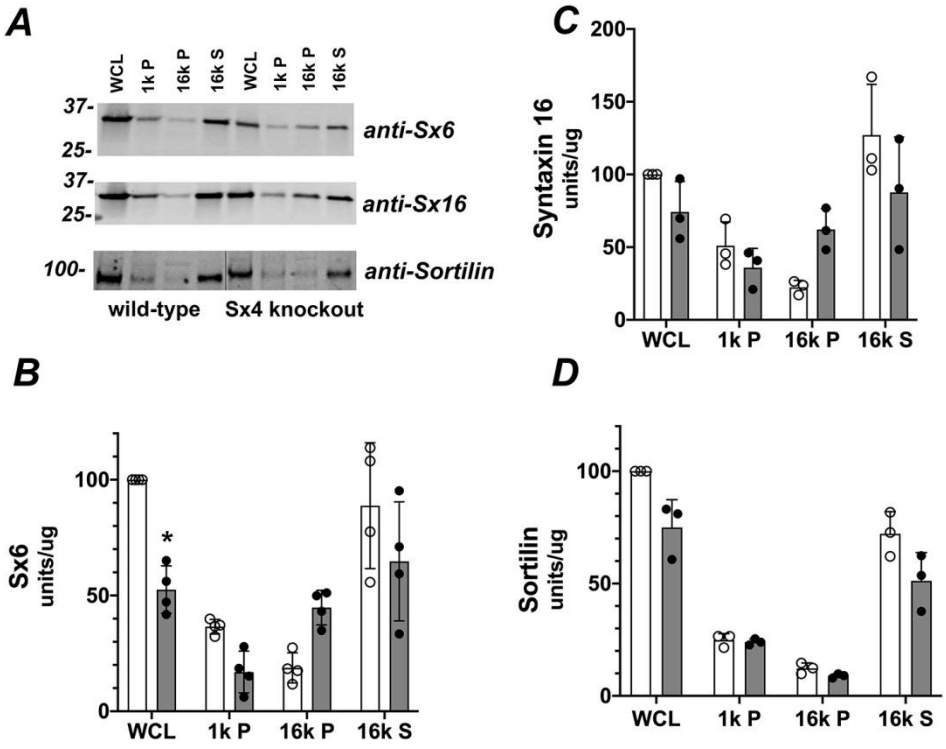

Figure 4. Sx6, 16 and sortilin levels are unchanged in Sx4 knockout cells.

Panel ***A*** shows representative immunoblots of subcellular fractions (as described in Fig. 1) from a single set of wild-type or Sx4 knockout 3T3-L1 adipocytes probed for the indicated proteins. Equal amounts of each fraction were loaded on each lane. Note that in the anti-sortilin blot shown, an empty lane has been removed (indicated by the black line) to facilitate comparison with other immunoblots from this data set. Quantification of separate immunoblots of this type from three separate plating of cells are shown in panel ***B*** (Sx6) ***C*** (Sx16) and ***D*** (sortilin). Differences between wild-type and Sx4 knockout cells did not reach significance for any fraction/protein, except for a reduction in Sx6 content in Sx4 knockout cells compared to wild-type (*p=0.001 in panel ***B***).

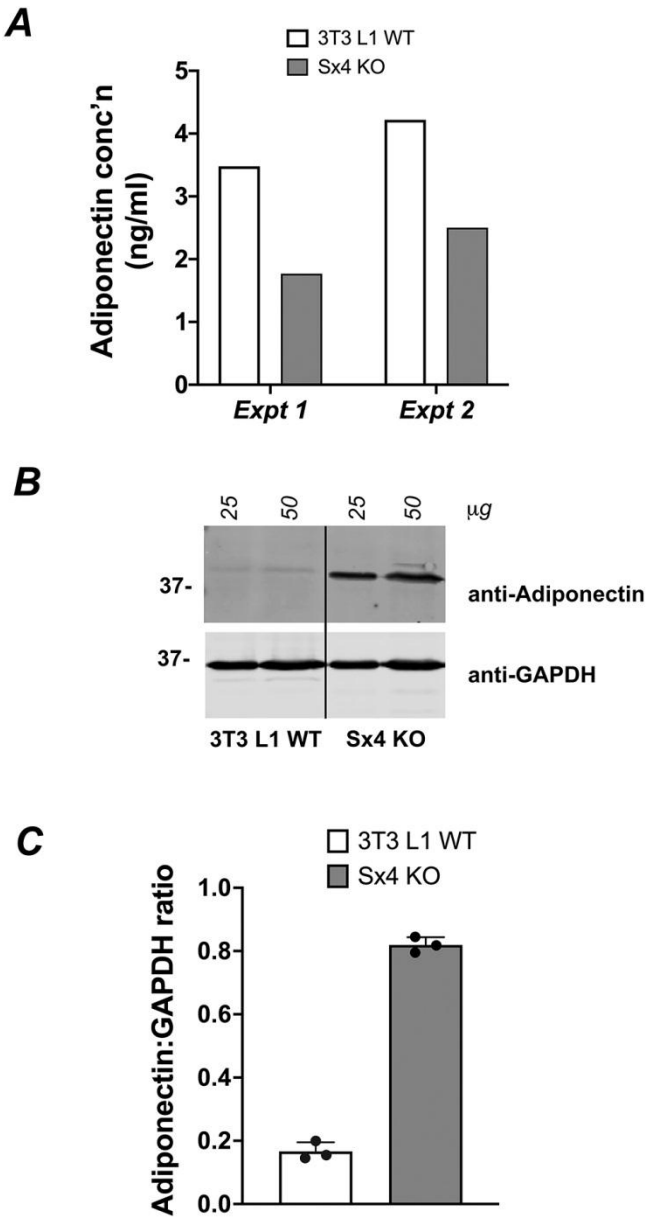

Figure 5. Adiponectin secretion is impaired in Sx4 knockout cells.

Panel ***A*** shows the results of ELISA assay measuring adiponectin released from wild-type or Sx4 knockout cells during 24h incubation in serum-free media. Data from two independent assays is shown, with each value representing triplicate measurements at each condition; note that multiple assays were performed using a range of volumes of supernatant to ensure linearity and reproducibility, but a single point is shown here for clarity. In Panel ***B*** either wild-type or Sx4 knockout cells were incubated in serum-free media for 24h and cell lysates prepared. Lysates were immunoblotted for anti-adiponectin or anti-GAPDH as indicated, with either 25 or 50 µg of protein loaded per lane as shown. Note that the blot shown had irrelevant lanes removed (indicated by the solid black line). Quantification of 3 experiments shown in Panel ***C***. The difference in adiponectin/GAPDH ratio in Sx4 knockout and wild-type cells was significant, p=0.001.

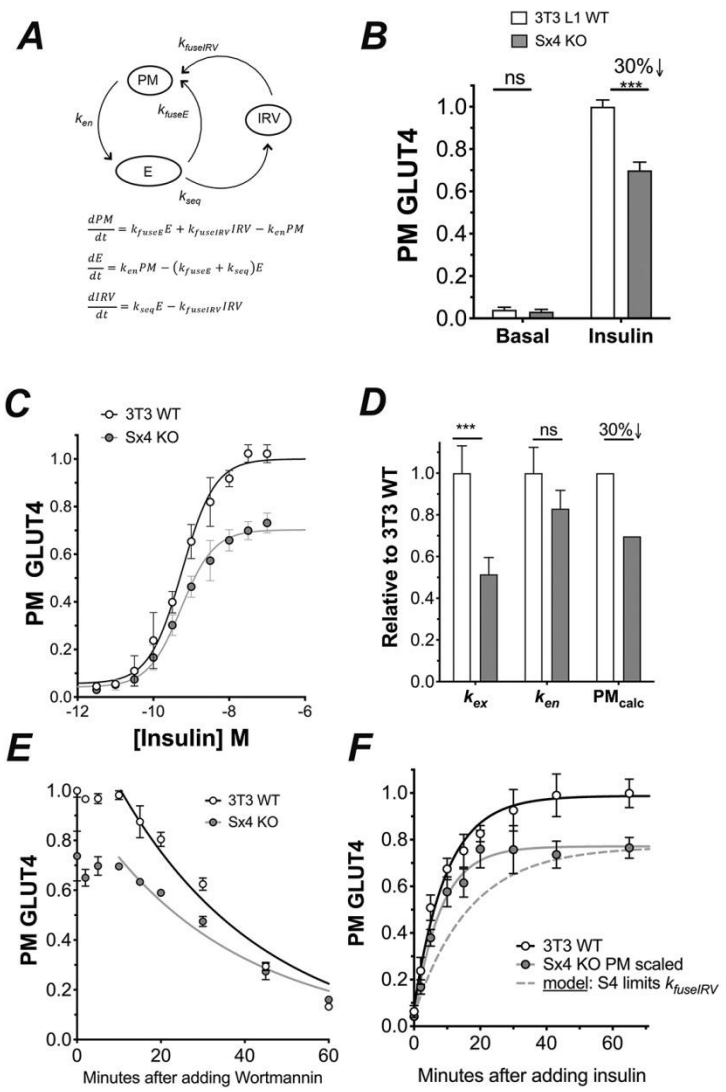

Figure 6. Recycling of ectopic HA-GLUT4-GFP in Sx4 knockout cells.

Panel ***A*** is a schematic of the model of GLUT4 recycling used. GLUT4 is shown to traffic between the plasma membrane (PM), endosomes (E) and the GSC/IRV (IRV)(Habtemichael et al., 2011; Muretta et al., 2008). The rate constants for each step are shown. Panel ***B*** shows the level of GLUT4 at the plasma membrane in the presence and absence of insulin (100 nM, 45 minutes). There is a 30% reduction in cell surface GLUT4 levels in Sx4 knockout cells compared to control; the mean + s.d. of 6 independent experiments is shown (***p<0.001 by ANOVA). No significant effect on basal levels was observed (n.s.). Panel ***C*** shows the effect of insulin on cell surface GLUT4 levels. The EC_{50} values of control and Sx4 knockout cells were 0.54 v 0.57 nM, respectively. The data shown is from 4 independent experiments. Panel ***D*** shows kinetic parameters, determined as outlined in *Methods* assayed in control and Sx4 knockout cells. A statistically significant 50% decrease in k_{ex} was observed (***p=0.004 by non-linear fit analysis) with no effect on k_{en}. When fitted to the model shown in Panel A, a 30% decrease in insulin stimulated GLUT4 levels at the PM in Sx4 knockout cells relative to control cells is predicted (PM_{calc}). Panel ***E*** shows the time-course of the decline in PM GLUT4 levels upon wortmannin (100nM) addition; cells were pre-treated with insulin for 45 min wortmannin added for the times shown before assay of cell surface GLUT4. The

rate constant of endocytosis, k_{en}, is unchanged (n=4 independent experiments). Panel ***F*** shows the half-time of the increase in relative surface GLUT4 in response to insulin; this was not significantly changed in Sx4 knockout cells relative to wild-type cells (mean + s.d. of n=4 independent experiments). The dashed line shows the result predicted if Sx4 was rate limiting for fusion of IRVs with the PM. Similar levels of HA-GLUT4-GFP were expressed in both wild-type and Sx4 knockout cells as judged by GFP fluorescence levels (not shown).

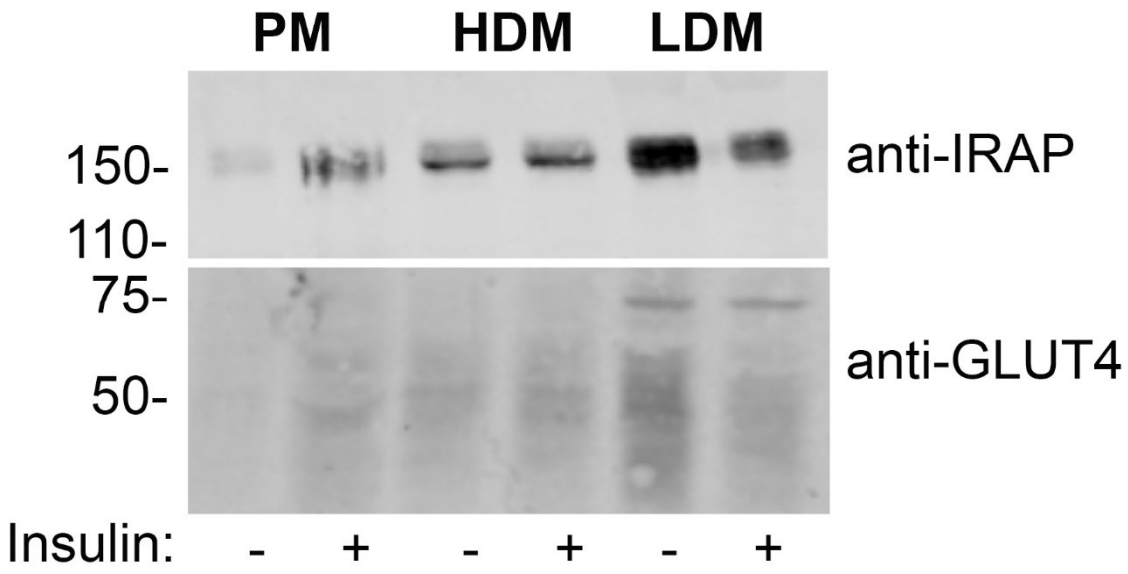

Fig. S1. IRAP exhibits insulin-stimulated translocation in Sx4 knockout cells.

Sx4 knockout adipocytes were incubated with or without 100 nM insulin for 20 minutes prior to subcellular fractionation as outlined (Sadler et al, 2015). Fractions enriched in plasma membranes (PM), high density microsomes (HDM) and low density microsomes (LDM) were generated, and equal fractions separated on SDS-PAGE and immunoblotted for levels of IRAP and GLUT4 as indicated. The data show that IRAP exhibits robust translocation from the LDM fraction to the PM fraction in response to insulin. Data shown from a representative experiment, replicated three times with qualitatively similar results. The approximate position of molecular weight markers is presented (in kDa).

Sadler, J.B.A., Bryant, N.J., and Gould, G.W. (2015). Characterization of VAMP isoforms in 3T3-L1 adipocytes: implications for GLUT4 trafficking. Mol. Biol. Cell *26*, 530–536.